



ChemComm

Free-standing membranes from the chemical exfoliation of mesoporous amorphous titania thin film

Journal:	<i>ChemComm</i>
Manuscript ID	CC-COM-05-2021-002645.R1
Article Type:	Communication

SCHOLARONE™
Manuscripts

COMMUNICATION

Free-standing membranes from the chemical exfoliation of mesoporous amorphous titania thin film

Victor Malgras,^{*a} Yoshitaka Matsushita,^a Joel Henzie,^a Yoshiyuki Sugahara,^{b,c} Yusuke Yamauchi^{*a,c,d}

Received 00th January 20xx,
Accepted 00th January 20xx

DOI: 10.1039/x0xx00000x

Thin films are typically bound to their substrate, limiting their integration on rough, porous, curved or chemically/thermally sensitive surfaces. Instead of employing tedious and expensive back-etching processes, certain chemical routes can enable the exfoliation of such thin structures. Herein, we demonstrate that an alkaline treatment can exfoliate a hybrid thin film comprising amorphous titania embedded in well-ordered block-copolymer micelles, which can be redeposited elsewhere. We provide sufficient evidence of the preservation of pore ordering and the importance of neutralizing the solution to spare the system from the redissolution of the titania species.

Several studies have demonstrated the fabrication of mesoporous oxide films through self-assembled soft-templating approaches.^{1–4} Their high surface area, pore size, and ordering are properties that have applications in a wide range of applications, such as sensing,^{5,6} biomedical,⁷ catalysis,^{8–10} and self-cleaning coatings.¹¹ These films are of interest as processing¹² and morphology control are continuously improving.¹³ Recently, vertically oriented mesoporous TiO₂ films with long-range ordering have been fabricated by exploiting the unidirectional contraction of a cubic-centered pore geometry ($Im\bar{3}m$).¹⁴ This example highlights how the features of some nanostructured films are related to the substrate they are adhered to. There are instances, however, where transferring such films on a support with a non-planar surface can be useful; for example, a macroporous substrate for hierarchical filtration membrane

and concave electrodes of a battery. Some approaches can achieve free-standing mesoporous organo-silica films at the water/air interface¹⁵; however, the lack of subsequent demonstrations and implementations suggests that further processing may be challenging. Manipulating these thin free-standing films in liquid media can be rather challenging.¹⁶ Exfoliation-assisted transfer is a common practice for transferring graphene from the synthesis platform for characterization or device integration,^{17,18} where simple, inexpensive, and non-destructive methods are generally favored. Herein, we demonstrate that mesoporous amorphous titania films can be exfoliated from their Si substrate by using an alkaline treatment and further transferred onto a new substrate, while retaining its mesoporous morphology. This approach employs soft forces as tools to separate the substrate from the film: while the former is maintained, face down, at the air-water interface through capillarity, the latter is pulled downward by gravity. We also emphasize the importance of controlling the pH of the final solution before extracting the free-standing film, which helps preserving the Ti-O_x scaffold.

The as-synthesized mesoporous titania film, of thickness 100 nm (± 10 nm), was selected because of its toughness, long-range pore ordering, and the ability to contract and generate vertical porosity upon annealing, which presents promising aspects for nano-/microfiltration membrane technology (SEM and AFM images are shown in Fig. 1).¹⁴ In such systems, the predominant aqueous phase containing the Ti⁴⁺ species induces

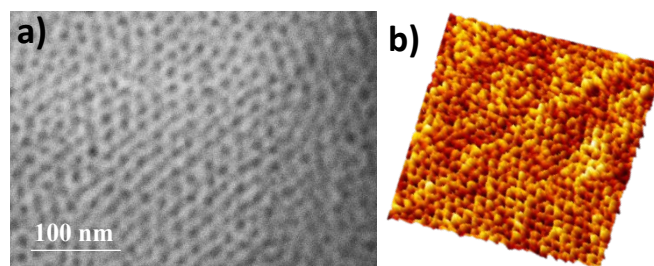


Fig. 1 a) SEM images of the mesoporous amorphous titania film (annealed at 150 °C) before exfoliation. b) AFM image of the mesoporous TiO₂ film annealed at 400 °C.

^a International Center for Young Scientists (ICYS) and Materials Nanoarchitectonics (MANA), National Institute for Materials Science (NIMS), 1-1 Namiki, Tsukuba, Ibaraki 305-0044, Japan.

^b Department of Applied Chemistry, School of Advanced Science and Engineering, Waseda University, 3-4-1 Okubo, Shinjuku, Tokyo 169-0085, Japan.

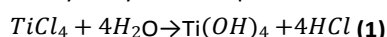
^c Kagami Memorial Research, Institute for Materials Science and Technology, Waseda University, 2-8-26 Nishiwaseda, Shinjuku, Tokyo 169-0051, Japan.

^d School of Chemical Engineering and Australian Institute for Bioengineering and Nanotechnology (AIBN), The University of Queensland, Brisbane, QLD 4072, Australia.

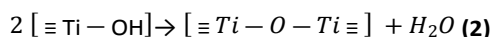
Electronic Supplementary Information (ESI) available: Experimental methods, XPS and XRD. See DOI: 10.1039/x0xx00000x

the formation of spherical micelles from the self-assembly of a polystyrene-*b*-poly(ethylene oxide) (PS-*b*-PEO) block copolymer, where the hydrophobic PS tails are oriented inside while the hydrophilic PEO heads remain outside to interact with water.

The presence of water can ensure, at least, partial hydration of the native SiO₂ layer, which lies above the silicon wafer, into silanol terminals (Si-OH). Because the PS blocks are allocated within the micelles, the adhesion of the film is expected to rely mostly on the hydrogen bonds (H-bonds) between the ether oxygen from the PEO blocks and the acidic silanol groups from the hydrated silica (Fig. 2, top-left).¹⁹ The hydrolysis reaction described by equation 1 is fast, resulting in low probability to observe titanium hydroxychloride species.²⁰

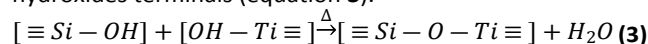


The condensation reaction (equation 2) can proceed slowly if performed in highly acidic aqueous media,²¹ however, it is generally completed rapidly during evaporation-induced self-assembly as the removal of water drives the process, resulting in amorphous titania, likely in the form TiO_x(OH)_y, embedded in polymeric micelles.



While the ether oxygen-silanol H-bonds take place immediately as the film is cast on the substrate, other adhesive interactions can arise from the inorganic components of the film after condensation, such as H-bonds between silanol and

Ti-OH or -O- terminals (Fig. 2, top-right). Deprotonation of anchoring H-bonds can be achieved using an alkaline agent, such as NaOH, to trigger the desorption of PEO and titanium oxyhydroxide species from the surface.^{22,23} Heating the film at temperatures higher than 100 °C was found to be necessary to consolidate the structure by triggering titania condensation, increasing the *x/y* ratio, and thus preventing complete dissolution during the alkaline treatment. Si-O-Ti bonds, are known to form at relatively low temperature,^{24,25} and can logically take place from the proximity of silanols and titanium hydroxides terminals (equation 3).



Beyond 150 °C, however, their abundant formation is expected to be responsible for firmly fastening the titania film to the substrate, thus suppressing subsequent exfoliation. The effect of temperature on the film integrity and exfoliability is described in more detailed in Fig. 2.

This approach was also experimented on films fabricated using Pluronic® poly(ethylene oxide)-*b*-poly(propylene oxide)-*b*-poly(ethylene oxide) F127 and P123 according to methods reported in references 4 and 26, respectively. In such case, despite the preliminary thermal treatment, the film whether dissolves (≤ 120 °C), or become insensitive to the alkaline exfoliation (≥ 150 °C), highlighting the importance of a sturdy and interconnected amorphous titania backbone. The ultra flat surface of Si and the weak interactions with silanol groups

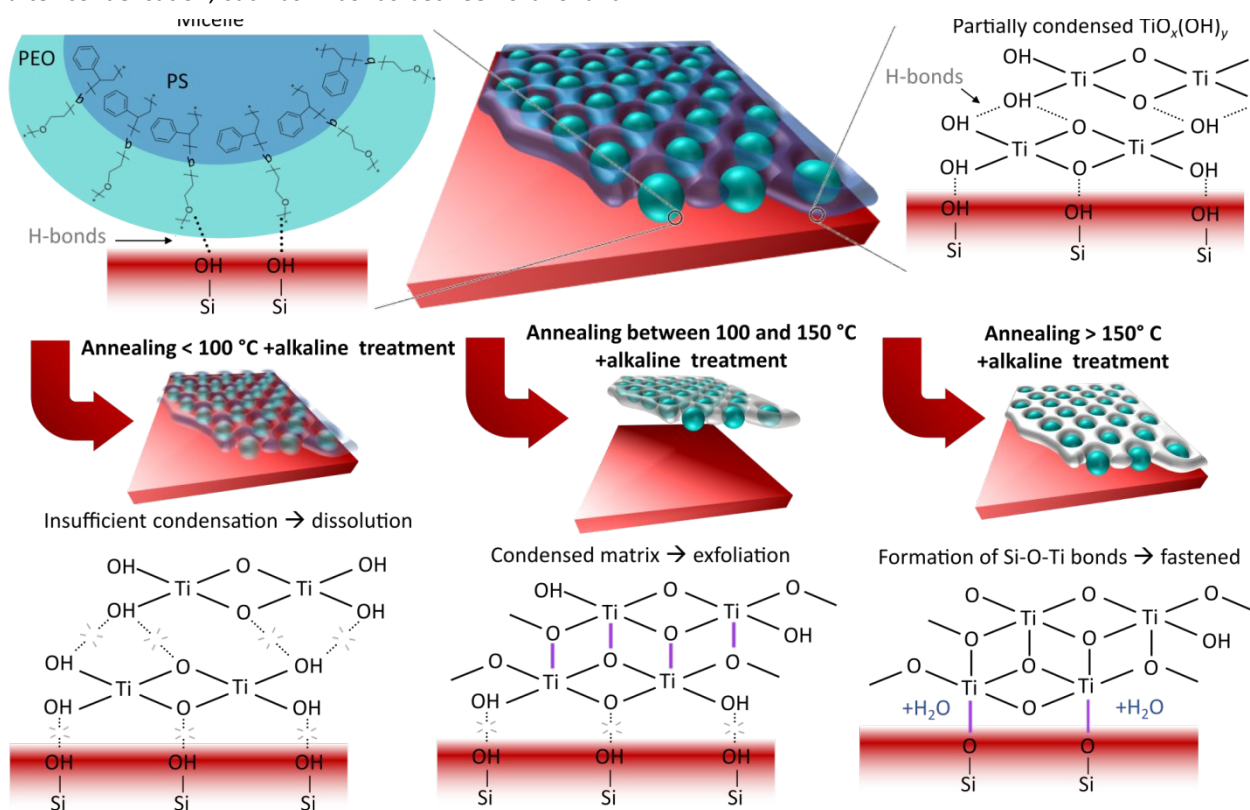


Fig. 2 Schematic illustration highlighting the major components responsible for adhering the film on the Si substrate. The film is composed of orderly packed spherical micelles embedded in partially condensed titania (top). N.B. A single micellar layer is represented for simplification, in reality 25 to 30 layers are stacked on one another. Briefly, H-bonds between silanol terminals and the PEO groups from the block copolymers (top left) as well as titanium oxyhydroxides (top right) are expected to accommodate adherence prior to any thermal treatment. Annealing at < 100 °C does not achieve sufficient condensation, thus alkaline treatment dissociates condensed domains and the film dissolves. Between 100 and 150 °C, the formation of larger Ti-O-Ti networks prevents dissolution, and exfoliation can take place as the H-bonds with the silanol terminals are weakened through deprotonation. Beyond 150 °C, exfoliation can no more be achieved due to the formation of abundant Si-O-Ti bonds fastening the TiO₂ scaffold on the substrate. The chemical configurations at the bottom illustrate the assumptions of bond breaking during alkaline treatment, and bond formation (in purple) during annealing.

appear to be critical factors enabling exfoliation, since other substrates with higher roughness and different surface chemistry, such as glass and ITO-coated glass, did not permit the release of the film.

Under optimal conditions, the film exfoliates within 30 min (Fig. 3a and videos in supplementary information) and can be collected on a substrate of choice, such as another Si chip. We selected a film with holes (from spin-coating defects) to show that patterns are kept intact and do not propagate during the exfoliation. The integrity of the mesoporous network was evaluated through TEM observation. Assuming that the free-standing membrane preserved the body-centered cubic $\text{Im}\bar{3}\text{m}$ porous structure ($a = 23.3 \text{ nm}$), the hexagonal and cubic patterns observed in Fig. 3b and c can be assigned to the (111) and (100) planes, respectively. It is believed that the inherent sturdiness of the parent mesoporous TiO_2 film is partially responsible for maintaining the pore structure during exfoliation. Grazing-incidence small-angle X-ray scattering (GI-SAXS) patterns of the film at the different stages of the process can be observed in Fig. 4, with a special focus on the in-plane ordering (white rectangle on the 2D patterns, inset). The as-deposited film annealed at 120°C exhibits a $d_{01\bar{1}}$ lattice of 16.3 nm , which is retained after exfoliation and redeposition. Following redeposition, two different annealing steps are applied in order to study their impact on pore-to-pore spacing. The shift induced by subsequent heating steps is assigned to a slight reduction of the $d_{01\bar{1}}$ lattice to 15.1 nm at 150°C and 14.6 nm at 400°C . While the former shift could be directly attributed to the loss of volume following water evaporation, the latter is more likely to be caused by crystallization-driven contractions. Annealing the as-deposited film, firmly attached to the substrate, has been reported to induce unidirectional contraction without affecting the lateral pore lattice,¹⁴ however, the loosely adhered membrane appears to undergo isotropic stress which could explain the shift observed. In addition, the expansion of the $01\bar{1}$ spot width and length along the semi-circular shape suggests a broader size distribution and a loss of verticality (e.g., slanted, tortuous), respectively.

The chemistry of the free-standing films was investigated by X-ray photoelectron spectroscopy (XPS) to understand the implications of annealing, exfoliation, and neutralization treatments on chemical coordination (O 1s and Ti 2p in Fig. 5, C 1s in Fig. S1, ESI[†]). In addition to the usual adventitious carbon, the contribution to the C 1s in the pristine sample is expected to include the organic skeleton still present in the film (as PS-*b*-PEO block copolymer). This participation is reduced after annealing treatments because of the removal of most aliphatic coordinated carbon and partial oxidation of remaining organic

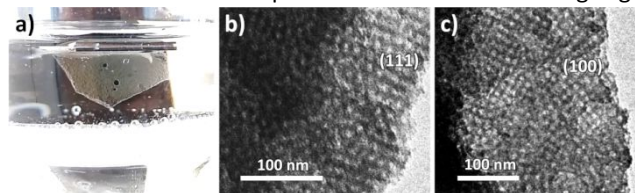


Fig. 3 a) Photograph of the amorphous titania film during exfoliation process. TEM images of the as-exfoliated free-standing film, exhibiting b) hexagonal ordering from the (111) plane and c) cubic ordering from the (100) plane of the $\text{Im}\bar{3}\text{m}$ structure.

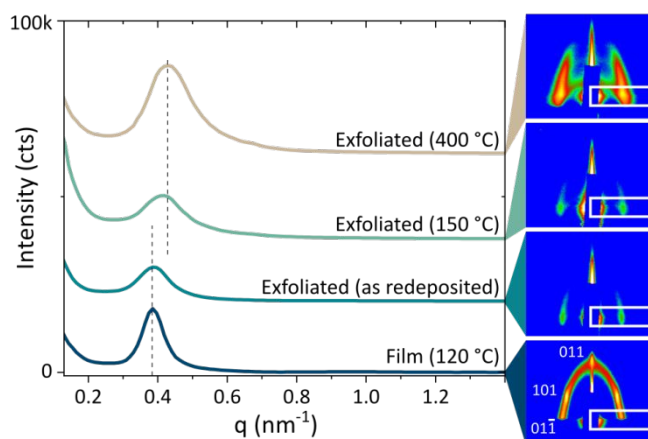


Fig. 4 SAXS patterns corresponding to the integration shown in the insets (right), highlighting the retained mesoporous structure and pore-to-pore distance.

moieties (shifted toward higher binding energies, at approximately 288.8 eV). This is accompanied by an increase in Ti-O_x contribution in the O 1s signal, observed at $\sim 530.5 \text{ eV}$, caused by the crystallization of TiO_2 . The increasing Ti 2p intensity is attributed to the significantly higher density in the TiO_2 crystal. After exfoliation, the alkaline treatment appears to disturb TiO_2 condensation during the final annealing step, as can be deduced from the loss of the Ti-O_x signal in both O 1s and Ti 2p contribution. This can be expected as under high-pH conditions (>14), excess concentration of OH^- can selectively dissolve amorphous titania from the surface, while sparing the bulk Ti-O-Ti network. The dissolution of titanate under basic conditions is at the core of the hydrothermal chemistry responsible for the formation of TiO_2 nanotubes.²⁷ The presence of Na in the exfoliated structure is confirmed from the strong Na 1s signal (Fig. S2, ESI[†]) at 1071.45 eV and can be attributed to the development of TiO-Na terminals, or the formation of NaCl crystals when the residual Cl^- ions (HCl) present in the sol film are immersed in the alkaline solution.

To circumvent this effect, we sought to alter the pH conditions so condensation can be favored within the vicinity of the isoelectric point of TiO_2 (pH 4.5 - 6.8).^{28,29} Therefore, an

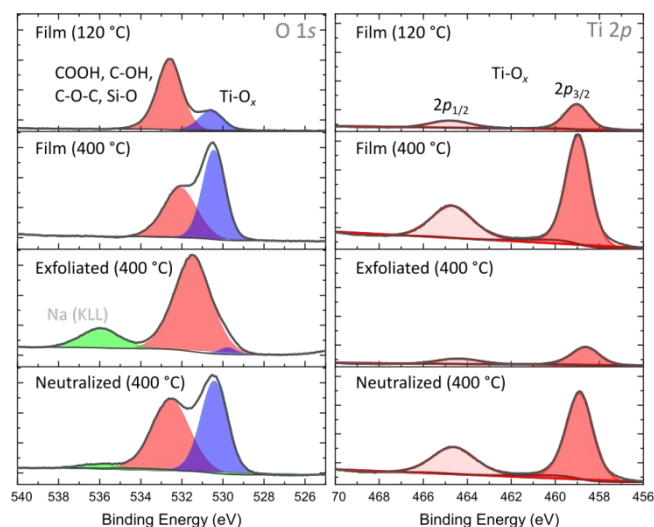


Fig. 5 XPS resolved around O 1s and Ti 2p for films annealed at 120 and 400°C , and exfoliated films without and with neutralization, followed by 400°C thermal treatment.

additional neutralization step is performed immediately following exfoliation, where 0.1 M HCl is added dropwise until neutral pH is reached. This should reduce considerably the concentration of OH⁻ responsible for dissolving the titania species. This has a critical impact on how the free-standing film condenses, as the Ti–O_x signal (O 1s and Ti 2p) is almost identical to the annealed film (unexfoliated). We also observe a dramatic reduction of the Na species contribution (1s and KLL), washed off by the acid neutralization (Fig. S2, ESI[†]). Finally, the weak C 1s intensity suggests that most organic compounds have been efficiently removed, and the resulting surface chemistry seems to limit the adsorption of adventitious carbons.

X-ray diffraction (XRD) was employed to assess the crystallization of each sample (Fig. S3, ESI[†]). Although the clear XPS signal confirms the presence of Ti–O_x in the neutralized sample after annealing, the crystallinity of TiO₂ cannot be detected by XRD. At this stage, it is impossible to confirm whether the crystallite size is confined below the diffraction detection limit (nanocrystalline, semicrystalline), or some other mechanism acts as crystallization inhibitor. Instead, the sharp reflections observed on the XRD pattern can be assigned to the Si substrate and to NaCl crystals, as previously suggested.

This study is a step forward to establish effective protocols to transfer mesoporous (semiconducting) oxides to different substrates (non-planar, chemically/thermally sensitive). Alkaline treatment is leveraged to break the hydrogen bonds responsible for the adhesion of the organic template/titania film on parent substrates. Such approach preserves the mesoporous structure and pore-to-pore distance, and the dissolution of Ti⁴⁺ can be inhibited through an additional neutralization step, however further work is necessary to optimize the chemistry driving the crystallization of TiO₂.

Acknowledgments

This work was supported by the JST-ERATO Yamauchi Materials Space-Tectonics Project (JPMJER2003), the Queensland Node of the Australian National Fabrication Facility (ANFF-Q), and the NIMS ICYS. TEM observations were carried out by the TEM station, XPS and XRD have been performed by the Surface Analysis Platform (NIMS).

Notes and references

- 1 H. Yang, A. Kuperman, N. Coombs, S. Mamiche-Afara and G. A. Ozin, *Nature*, 1996, **379**, 703–705.
- 2 Y. Lu, R. Ganguli, C. A. Drewien, M. T. Anderson, C. Jeffrey Brinker, W. Gong, Y. Guo, H. Soye, B. Dunn, M. H. Huang and J. I. Zink, *Nature*, 1997, **389**, 364–368.
- 3 D. Zhao, P. Yang, D. I. Margolese and G. D. Stucky, *Chem. Commun.*, 1998, 2499–2500.
- 4 D. Grosso, G. J. D. A. A. Soler-Illia, E. L. Crepaldi, F. Cagnol, C. Sinturel, A. Bourgeois, A. Brunet-Bruneau, H. Amenitsch, P. A. Albouy and C. Sanchez, *Chem. Mater.*, 2003, **15**, 4562–4570.
- 5 A. Walcarius, *Electroanalysis*, 2015, **27**, 1303–1340.
- 6 G. Wirnsberger, B. J. Scott and G. D. Stucky, *Chem.*

- 7 *Commun.*, 2001, 119–120.
- 8 Y. Liu, X. Wang, F. Yang and X. Yang, *Microporous Mesoporous Mater.*, 2008, **114**, 431–439.
- 9 E. Ortel, S. Sokolov, C. Zielke, I. Laueremann, S. Selve, K. Weh, B. Paul, J. Polte and R. Kraehnert, *Chem. Mater.*, 2012, **24**, 3828–3838.
- 10 M. Zirak, H. Oveisi, J. Lin, Y. Bando, A. A. Alshehri, J. Kim, Y. Ide, M. S. A. Hossain, V. Malgras and Y. Yamauchi, *Bull. Chem. Soc. Jpn.*, 2018, **91**, 1556–1560.
- 11 M. B. Zakaria, V. Malgras, T. Nagata, J. Kim, Y. Bando, A. Fatehmulla, A. M. Aldhafiri, W. A. Farooq, Y. Jikihara, T. Nakayama, Y. Yamauchi and J. Lin, *Microporous Mesoporous Mater.*, 2019, **288**, 109530.
- 12 B. Jin, J. He, L. Yao, Y. Zhang and J. Li, *ACS Appl. Mater. Interfaces*, 2017, **9**, 17466–17475.
- 13 D. R. Ceratti, B. Louis, X. Paquez, M. Faustini and D. Grosso, *Adv. Mater.*, 2015, **27**, 4958–4962.
- 14 R. R. Salunkhe, J. Lin, V. Malgras, S. X. Dou, J. H. Kim and Y. Yamauchi, *Nano Energy*, 2015, **11**, 211–218.
- 15 V. Malgras, Y. Shirai, T. Takei and Y. Yamauchi, *J. Am. Chem. Soc.*, 2020, **142**, 15815–15822.
- 16 H. Yang, N. Coombs, I. Sokolov and G. A. Ozin, *Nature*, 1996, **381**, 589–592.
- 17 J. W. Suk, A. Kitt, C. W. Magnuson, Y. Hao, S. Ahmed, J. An, A. K. Swan, B. B. Goldberg and R. S. Ruoff, *ACS Nano*, 2011, **5**, 6916–6924.
- 18 J. D. Wood, G. P. Doidge, E. A. Carrion, J. C. Koepke, J. A. Kaitz, I. Datye, A. Behnam, J. Hewaparakrama, B. Aruin, Y. Chen, H. Dong, R. T. Haasch, J. W. Lyding and E. Pop, *Nanotechnology*, 2015, **26**, 055302.
- 19 Y. Zhang, J. J. Magan and W. J. Blau, *Sci. Rep.*, 2015, **4**, 4822.
- 20 G. J. Fleer, in *Reagents in Mineral Technology*, eds. P. Somasundaran and B. M. Moudgil, Routledge, 2018, pp. 105–158.
- 21 T.-H. Wang, A. M. Navarrete-López, S. Li, D. A. Dixon and J. L. Gole, *J. Phys. Chem. A*, 2010, **114**, 7561–7570.
- 22 J. H. Lee and Y. S. Yang, *J. Eur. Ceram. Soc.*, 2005, **25**, 3573–3578.
- 23 J. Rubio and J. A. Kitchener, *J. Colloid Interface Sci.*, 1976, **57**, 132–142.
- 24 B. M. Lowe, C. K. Skylaris and N. G. Green, *J. Colloid Interface Sci.*, 2015, **451**, 231–244.
- 25 G. Sahasrabudhe, S. M. Rupich, J. Jhaveri, A. H. Berg, K. A. Nagamatsu, G. Man, Y. J. Chabal, A. Kahn, S. Wagner, J. C. Sturm and J. Schwartz, *J. Am. Chem. Soc.*, 2015, **137**, 14842–14845.
- 26 Y. Liu, J. Zhang, H. Wu, W. Cui, R. Wang, K. Ding, S.-T. Lee and B. Sun, *Nano Energy*, 2017, **34**, 257–263.
- 27 C. Wu, T. Ohsuna, M. Kuwabara and K. Kuroda, *J. Am. Chem. Soc.*, 2006, **128**, 4544–4545.
- 28 D. V. Bavykin, V. N. Parmon, A. A. Lapkin and F. C. Walsh, *J. Mater. Chem.*, 2004, **14**, 3370–3377.
- 29 M. Anpo, in *Studies in Surface Science and Catalysis*, 2000, pp. 157–166.
- 30 D.-S. Lee and T.-K. Liu, *J. Sol-Gel Sci. Technol.*, 2002, **25**, 121–136.